MAX-PLANCK-INSTITUT FÜR PLASMAPHYSIK

GARCHING BEI MÜNCHEN

CALCULATED TRAPPING CURVES OF D IN C AND Si

W. Eckstein

IPP 9/33 October 1980

Die nachstehende Arbeit wurde im Rahmen des Vertrages zwischen dem Max-Planck-Institut für Plasmaphysik und der Europäischen Atomgemeinschaft über die Zusammenarbeit auf dem Gebiete der Plasmaphysik durchgeführt.

IPP 9/33 W. ECKSTEIN CALCULATED TRAPPING CURVES OF D IN C AND Si

October 1980

ABSTRACT

The trapping of deuterium in solids is investigated with the Monte Carlo program TRIM. The amount of deuterium trapped in amorphous carbon and silicon exposed to a plasma is calculated as a function of incident fluence and plasma temperature. These data can be used to obtain plasma parameters from measured trapping curves on probes exposed to a plasma.

1. INTRODUCTION

The implantation of hydrogen into the vacuum vessel wall is an important process in plasma machines /1, 2/. The energies and the angles with which the particles bombard the wall are dependent on the conditions of the plasma edge. It was the idea of Staudenmaier and Staib to get information of the plasma edge temperature and about the particle flux to the wall by measuring the trapped amount of hydrogen probes exposed to a plasma /3-5/. To reach this goal it is necessary to know the trapping curves for the hydrogen bombardment with a broad energy and angular distribution. This is difficult to establish experimentally, but it is possible to use a Monte Carlo program, here TRIM /6/, to calculate range distributions of hydrogen in carbon and silicon and with the knowledge of experimentally determined saturation concentrations the corresponding trapping curves can be obtained. For mono-energetic implantation trapping curves and depth distributions can be compared with experimental results to check the calculations /7-9/. A further advantage of the calculations is the applicability to low energies where no experimental results are available. Carbon and silicon have been used so far because there is no indication of diffusion of hydrogen in these materials at room temperature. All calculations are performed for deuterium, since there are only scarce experimental data for hydrogen.

2. MODEL

The depth distributions of the implanted deuterium are calculated by the TRIM program /6/. The TRIM program is based on the binary collision model as many other codes. The particles loose their energy mainly by inelastic collisions and the trajectory is determined by nuclear collisions. Two inelastic energy loss models are used:

the Lindhard-Scharff(LS) /10/ and the Oen-Robinson (OR) inelastic energy loss /11/. The Molière-potential is used for determining the deflections by elastic collisions. The particles are followed until they have slowed down to an energy of 5 eV. The program does not include any chemical effects or diffusion in the solid.

For the determination of the trapping curves (the amount of deuterium atoms trapped per cm^2 as a function of the incident fluence) the calculated depth distribution is linearly increased until the maximum of the depth distribution has reached the given saturation concentration of deuterium in the solid. Up to this point the trapping curve is linear with fluence. With a further increase of primary fluence particles are only trapped at depths, where saturation has not yet been reached. In this procedure it is assumed that the depth distribution for a given incident energy does not change with dose as long as the trapped amount at a certain depth is below the saturation concentration. For monoenergetic bombardment the calculated trapping curves can be checked by experimental results /3/. The same kind of procedure has been used by Cohen and McCracken /12/ to construct trapping curves, but with the difference that they used Gaussian depth distributions with ranges taken from Brice code /13/ calculations.

For applications in plasma machines an isotropic Maxwellian velocity distribution was assumed. The ion flux $\Gamma_{\parallel}$ per unit density parallel to the magnetic field lines onto a probe perpendicular to the magnetic field $\vec{B}$ is then given by

$$d\Gamma_{\parallel} = \frac{dn}{n_o} v_{\parallel} = \sqrt{\frac{2}{\pi}} \left(\frac{E}{m}\right)^{1/2} \cdot \frac{E}{E'} \exp\left(-\frac{E}{E'}\right) d\left(\frac{E}{E'}\right) \sin\alpha \cos\alpha \, d\alpha \quad (1)$$

with $E' = kT$, m = ion mass, $v_{\parallel}$ = ion velocity parallel $\vec{B}$, α = angle of incidence and n_o = plasma density. The depth distribution $D(x)$ for the flux given in (1) can be written in the following way:

$$D(x) = \int_0^{E_{max}} \int_0^{90^\circ} D(x,E,\alpha)\, d\Gamma_{\parallel} = \int_0^{E_{max}} \int_0^{90^\circ} D(x,E,\alpha) f(E) g(\alpha)\, dE d\alpha \qquad (2)$$

where $D(x,E,\alpha)$ is the depth distribution for the incident energy E and an angle of incidence α. x is the depth normal to the surface. Dividing up the integrals in a sum of integrals and subsequent integration yields:

$$D(x) = \sum_i \sum_j D(x,\bar{E}_i,\bar{\alpha}_j) f_1(\bar{E}_i) f_2(\bar{\alpha}_j) \qquad (3)$$

with

$$f_1(\bar{E}_i) = \sqrt{\frac{2}{\pi}} \left(\frac{E'}{m}\right)\left[\left(1 + \frac{E_i}{E'}\right)\exp\left(-\frac{E_i}{E'}\right) - \left(1 + \frac{E_{i+1}}{E'}\right)\exp\left(-\frac{E_{i+1}}{E'}\right)\right] \qquad (4a)$$

$$f_2(\bar{\alpha}_j) = \frac{1}{2}\left(\sin^2\alpha_{j+1} - \sin^2\alpha_j\right) \qquad (4b)$$

and

$$\bar{E}_i = (E_{i+1} + E_i)/2$$

$$\bar{\alpha}_j = (\alpha_{j+1} + \alpha_j)/2$$

$D(x,E,\alpha)$ is assumed to be constant in the intervals $(E_i - E_{i+1})$ and $(\alpha_j - \alpha_{j+1})$.

The depth distributions $D(x,\bar{E}_i,\bar{\alpha}_j)$ are calculated for 15 incident energies $\bar{E}_i$ ($\bar{E}_i$ = 10, 30, 50, 70, 90, 150, 250, 350, 450, 550, 650, 750, 850, 950 and 1500 eV) and for 10 angles of incidence $\bar{\alpha}_j$ ($\bar{\alpha}_j = 2.5^\circ$; 10°; 20°; 30°;

40^{o}; 50^{o}; 60^{o}; 70^{o}; 80^{o}; $87{,}5^{o}$). For each $(\bar{E}_j, \bar{\alpha}_j)$-combination 20000 incident particles were used. E_{max} was chosen to be 2 keV.
The depth distributions weighted with the known factors f_1 and f_2 are added together. Then the same procedure as for the monoenergetic distributions is applied to get the corresponding trapping curves.

The calculated depth distributions are stored on tape so that trapping curves for other saturation concentrations and plasma temperatures can easily be determined.

3. RESULTS

Calculations have been done for implantation of D in amorphous C and Si. For carbon only the Lindhard-Scharff (LS) /10/ inelastic energy loss $\Delta E_{LS} = C \cdot k_L \cdot \sqrt{E}$ with the correction factor C = 1.0 has been applied. For Si both the LS value with C = 1.6 as well as the Oen-Robinson (OR) /11/ local inelastic energy loss $\Delta E_{OR} = E_{LS} \cdot 0.045 \cdot \exp(-0.3 \cdot r/a) / (\pi a^2)$ with C = 1.7 has been used. The Oen-Robinson energy loss is always used for Si if it is not stated otherwise. This choice gave the best agreement with experimental results /7/. For both targets the saturation concentration was chosen to be 40 % /13,3/.

Depth distributions for monoenergetic implantations and for three angles of incidence are shown in fig.1-3 for D in C and in figs. 4-6 for D in Si. The shape of the distributions is changing with the angle of incidence α: With increasing α the maxima shift nearer to the surface, the width of the distributions gets slightly smaller and the implanted number of particles decreases. The depth distributions become broader with increasing incident energy E_o.

As a measure for the shape of the depth distributions the average depth $\bar{x}$ normal to the surface (mean projected range) which is the first moment of the distribution, and the standard deviation of the average depth $(x^2-\bar{x}^2)^{1/2}$, which is the second moment of the distribution, are shown in figs.7 and 8 for D in C and in figs.9 and 10 for D in Si as a function of cos α. These figures clearly demonstrate that the average depth is not proportional to cos α, but that the dependence on the angle of incidence is rather small at least for energies below a few hundred eV. Also the standard deviation of the average depth shows only a small dependence on α. It should be mentioned that the average depth is <u>not</u> the position of the maximum of the distribution and that the standard deviation of the average depth differs from the half width of the distributions.

The average depth and the standard deviation of the average depth versus the incident energy E_o for $\alpha = o$ are given in fig.11 for D in C and in fig.12 for D in Si. In these log-log plots the average depth is nearly a straight line, corresponding to a power law $\bar{x} \sim E^c$ with c slightly below 1. The calculated curves might shift up or down somewhat for different values of the inelastic energy loss and the interaction potential.

Depth distributions of implanted D in amorphous C and Si for a Maxwellian energy distribution and an isotropic angular distribution of the incident ions are shown in the figs.13-14. Parameter at these curves is the ion temperature kT. The distributions exhibit an exponential decrease at least for part of the distribution.

These depth distributions have been used to calculate trapping curves in a similar way as for monoenergetic implantations, i.e. trapping at each depth until the saturation concentration is reached. In the following figs. 15-20 the calculated trapping curves for D in C and Si are shown. The monoenergetic curves have been included here because they can be checked experimentally. For Si two different inelastic energy losses 1.6 times the Lindhard-Scharff (fig.17) and 1.7 times the Oen-Robinson value (fig.18), have been used to show the dependence of the trapping curves on one of the important parameters which enter the calculations. From comparison with experimental data (monoenergetic implantation) the second case (fig.18) yielded better agreement with measured depth distributions /9/. For a different saturation concentration the trapping curves are not changed in the linear part, but the trapped amount at high fluences is increased proportional to the saturation concentration as can be seen by comparing figs. 19-20.

In order to get a feeling about the dependence of the reflection on the angle of incidence the particle reflection coefficient versus the angle of incidence α are given in figs.21 and 22 for D on C and Si for a few incident energies.

4. DISCUSSION

The model to construct the trapping curves is based on Monte Carlo calculations of the depth distribution with the program TRIM. TRIM has been tested for a large variety of scattering and implantation problems and TRIM results gave reasonable agreement with experimental results at least for energies above a few hundred eV (see for example /14/. But it should be kept in mind that

these calculations are based on the binary collision model. It is not clear at which energies this assumption breaks down, but it seems to work even at energies of about 10 eV as the application of this code to sputtering problems indicate. Chemical effects which may become important at low energies are not included in the code. Other uncertainties are the potential and the inelastic stopping used in the code. Especially there are no experimental data for energies below 1 keV for the inelastic energy loss. One has to rely on theoretical models as Lindhard-Scharff's, Oen-Robinson's or Firsov's approaches. The program deals with an ideally flat surface which might not be the case in the experiments. Surface roughness, oxide layers and implanted gas tend to increase the trapped amount /15/. Swelling of the implanted material may also change the results /9/.

The trapping curves published in /12/ are in good overall agreement with the results given in this report, but there are some systematic deviations; especially the linear part of the trapping curves is shifted to higher fluences in /12/.

ACKNOWLEDGEMENT

The author likes to thank J. Biersack for the possibility to use the TRIM program. The topic of this report was triggered by G. Staudenmaier. Many discussions with him and W. Poschenrieder helped to clarify the problems. Many thanks are due to Mrs. Walter who did most of the programming.

REFERENCES

/1/ G.M. McCracken, J.Nucl.Mat. 85&86 (1979) 943

/2/ R. Behrisch, J. Phys.(France) 38 (1977), C 3

/3/ G. Staudenmaier, J.Roth, R.Behrisch, J. Bohdansky, W. Eckstein, P.Staib, S.Matteson and S.K.Erents, J.Nucl.Mat.84 (1979) 149

/4/ TFR Group, Bull.Am.Phys.Soc. 23 (1978) 802

/5/ G.Staudenmaier, P. Staib and R. Behrisch, Nucl.Fusion 20 (1980) 96

/6/ J.P. Biersack and L.G. Haggmark, to be published

/7/ W. Eckstein, K. Wittmaack to be published

/8/ C.W. Magee, S.A. Cohen, D.E.Voss and D.K.Brice, Nucl.Instr.Meth.168 (1980)383

/9/ K. Wittmaack and G.Staudenmaier, 4th Int.Conf. Plasma Surface Interactions in Contr.Fusion Devices, Garmisch April 1980, to be published in J. Nucl.Mat.

/10/ J. Lindhard and M.Scharff, Phys.Rev. 124 (1961)128

/11/ O.S. Oen and M.T. Robinson, Nucl.Instr.Meth.132 (1976) 647

/12/ S.A.Cohen and G.M.McCracken, J.Nucl.Mat. 84 (1979)157

/13/ D.K. Brice, Rad.Eff.13(1972) 215

/14/ J.Roth, B.M.U.Scherzer, R.S.Blewer, D.K.Brice, S.T.Picraux and W.R.Wampler, J.Nucl.Mat. 94&95 (1980).

/15/ W.Eckstein, H.Verbeek, IPP-Report 9/32, August 1979

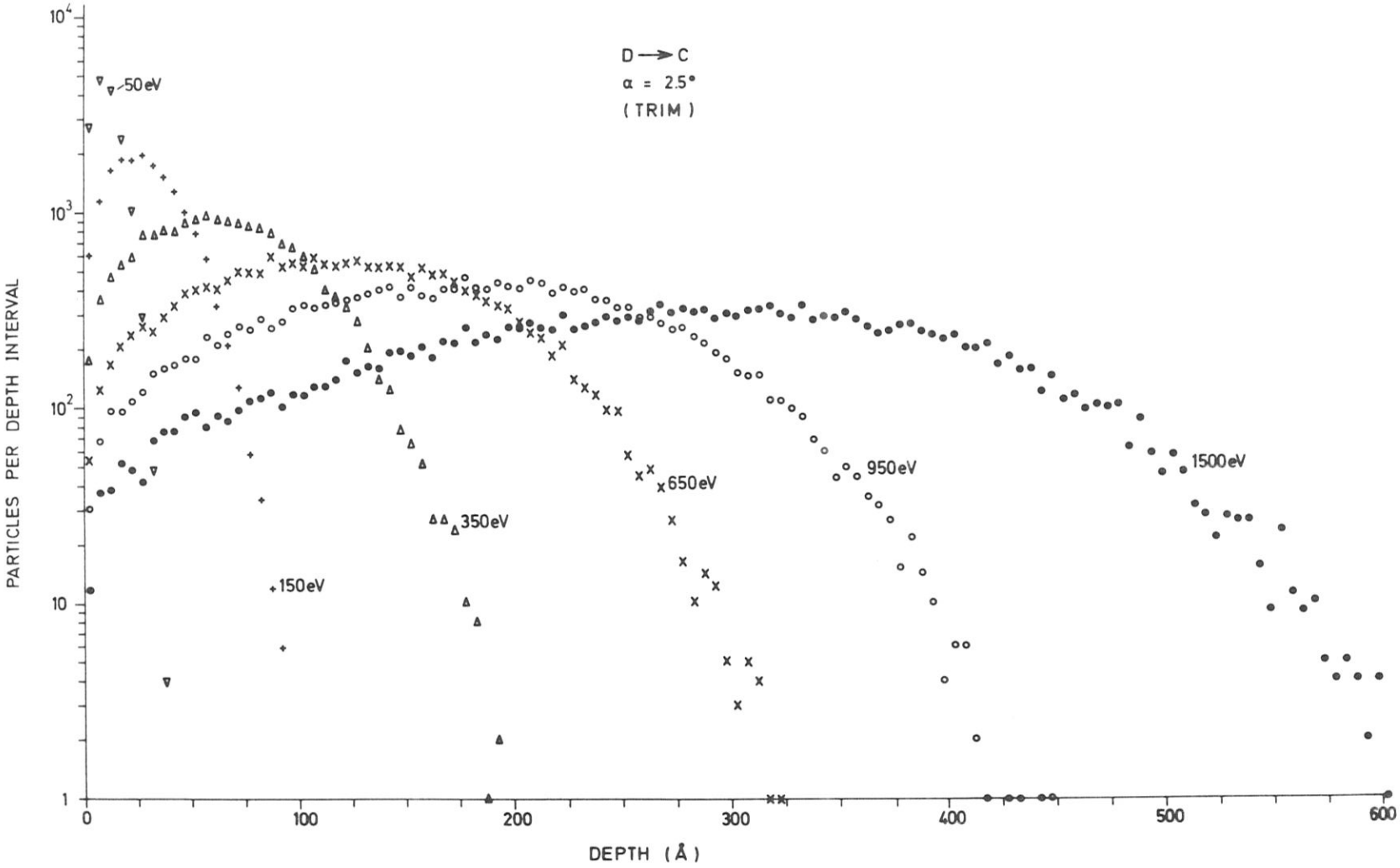

Fig.1: Depth distributions of implanted D in C for 6 incident energies and an angle of incidence $\alpha = 2.5^{o}$ (in respect to the surface normal), the number of incident particles are 20 000 for one incident energy, the depth interval is 5 Å. Lindhard inelastic energy loss was assumed.

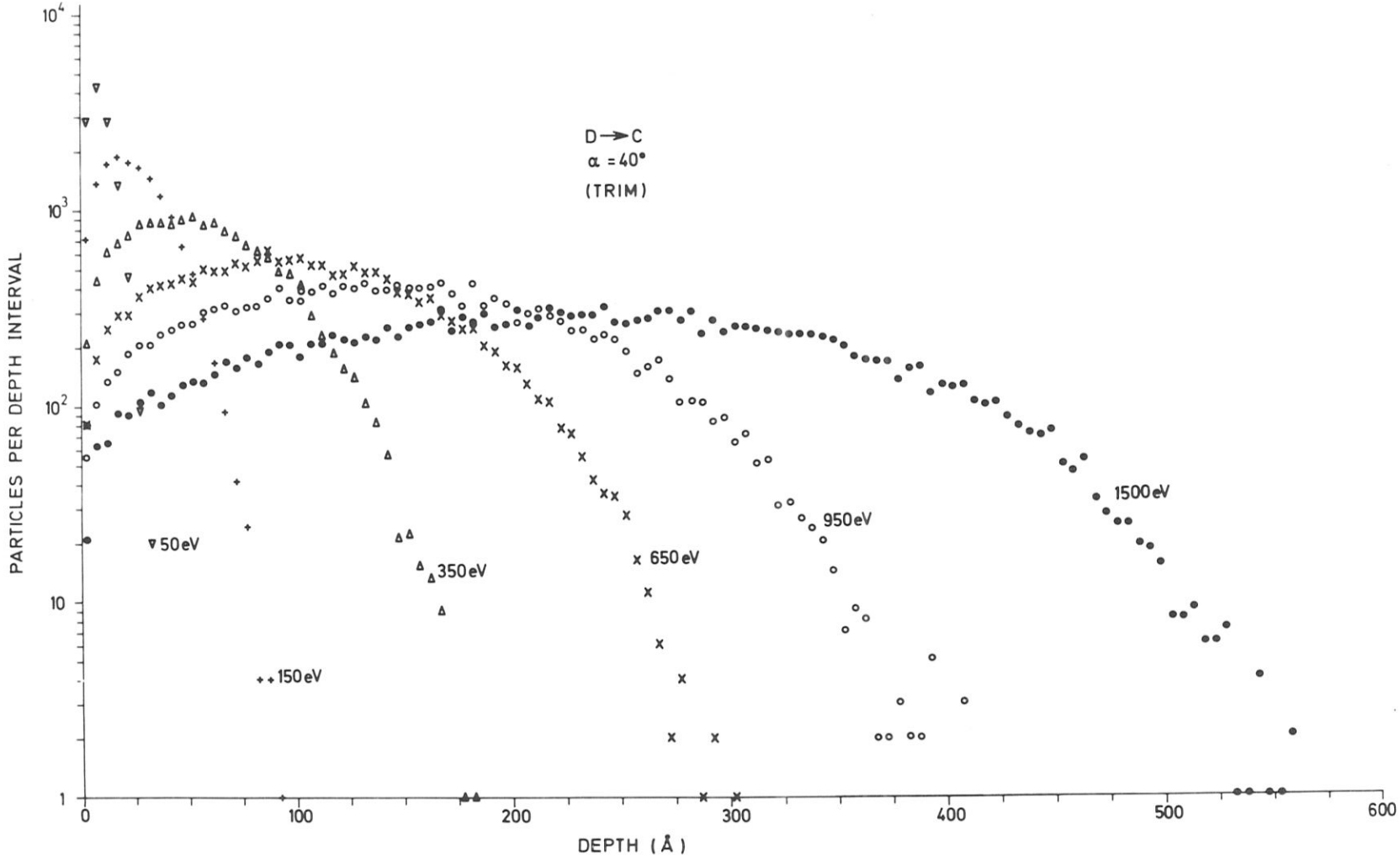

Fig.2: Depth distributions of implanted D in C for 6 incident energies and an angle of incidence $\alpha = 40^{o}$ (in respect to the surface normal). The number of incident particles are 20 000 for one incident energy, the depth interval is 5 Å. Lindhard inelastic energy loss was assumed.

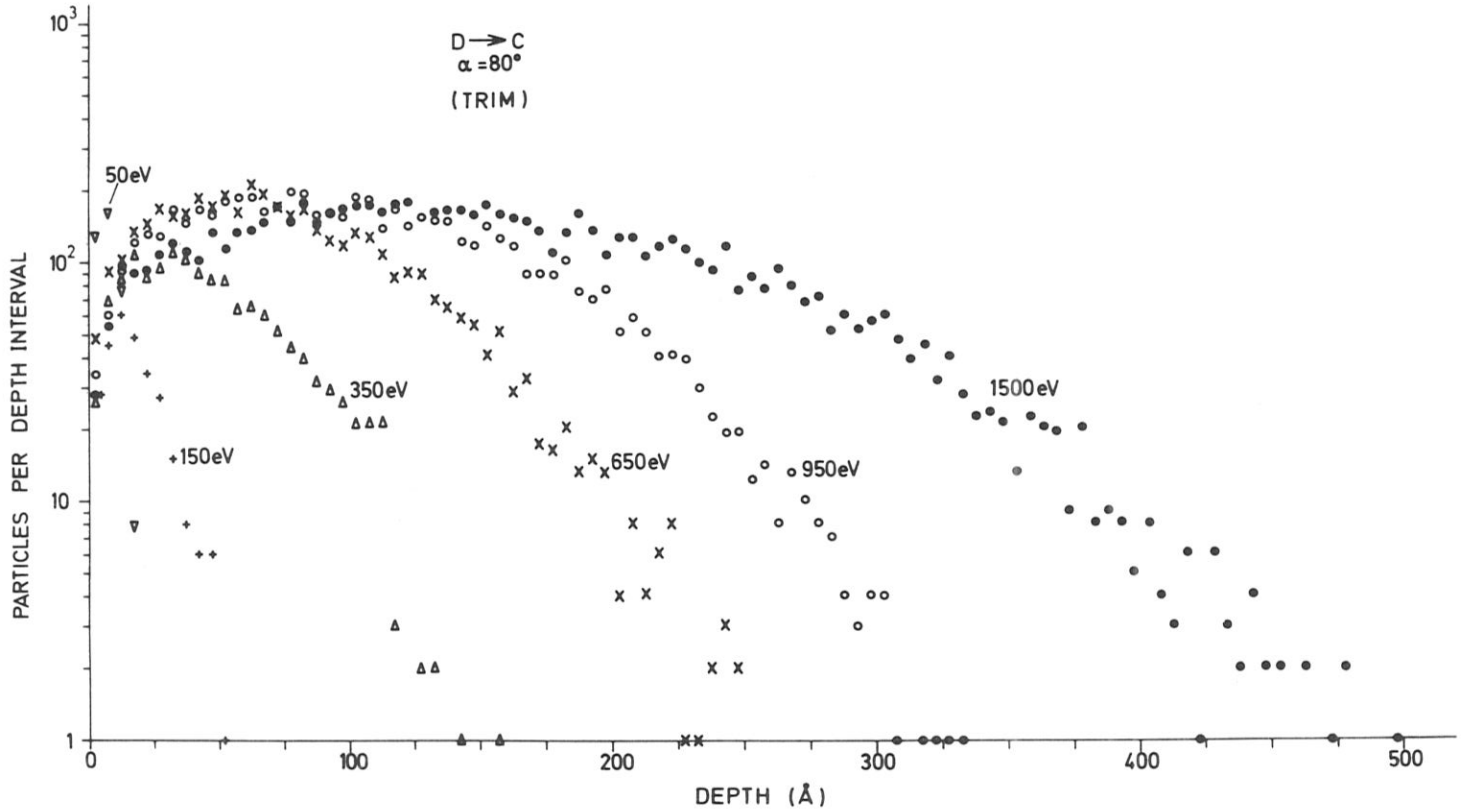

Fig.3: Depth distributions of implanted D in C for 6 incident energies and an angle of incidence $\alpha = 80^{o}$ (in respect to the surface normal). The number of incident particles are 20 000 for one incident energy, the depth interval is 5 Å. Lindhard inelastic energy loss was assumed.

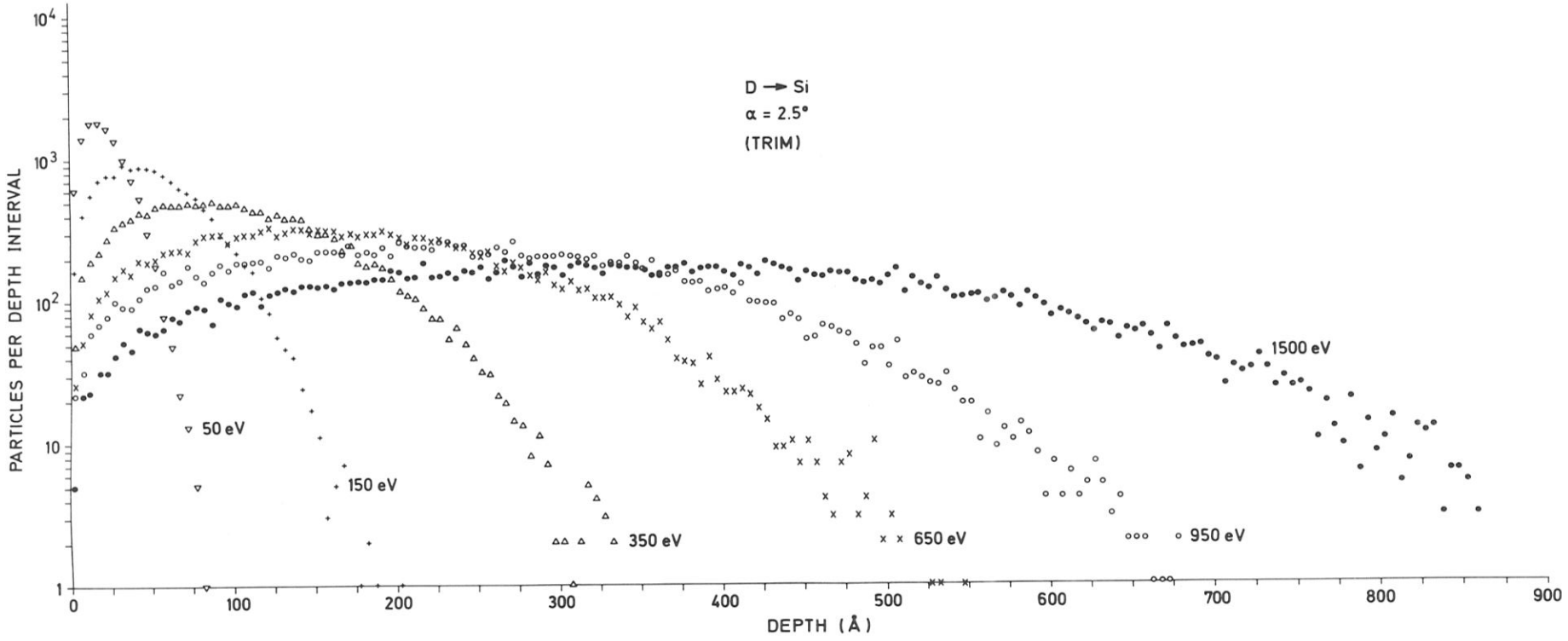

Fig.4: Depth distributions of implanted D in Si for 6 incident energies and an angle of incidence $\alpha = 2.5^{o}$ (in respect to the surface normal). The number of incident particles are 20 000 for one incident energy, the depth interval is 5 Å. 1.7 x Oen-Robinson inelastic energy loss was assumed.

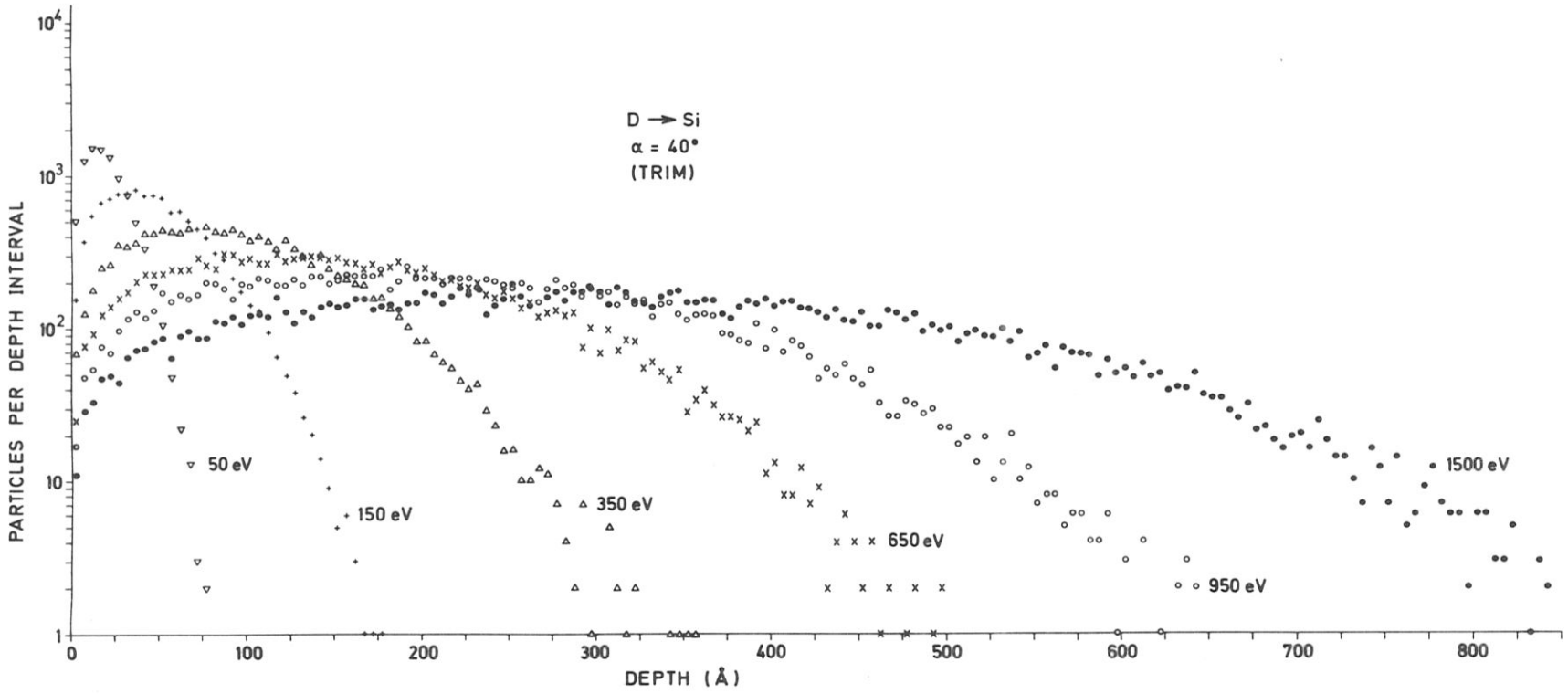

Fig.5: Depth distributions of implanted D in Si for 6 incident energies and an angle of incidence $\alpha = 40^{o}$ (in respect to the surface normal). The number of incident particles are 20 000 for one incident energy, the depth interval is 5 Å. 1.7 x Oen-Robinson inelastic energy loss was assumed.

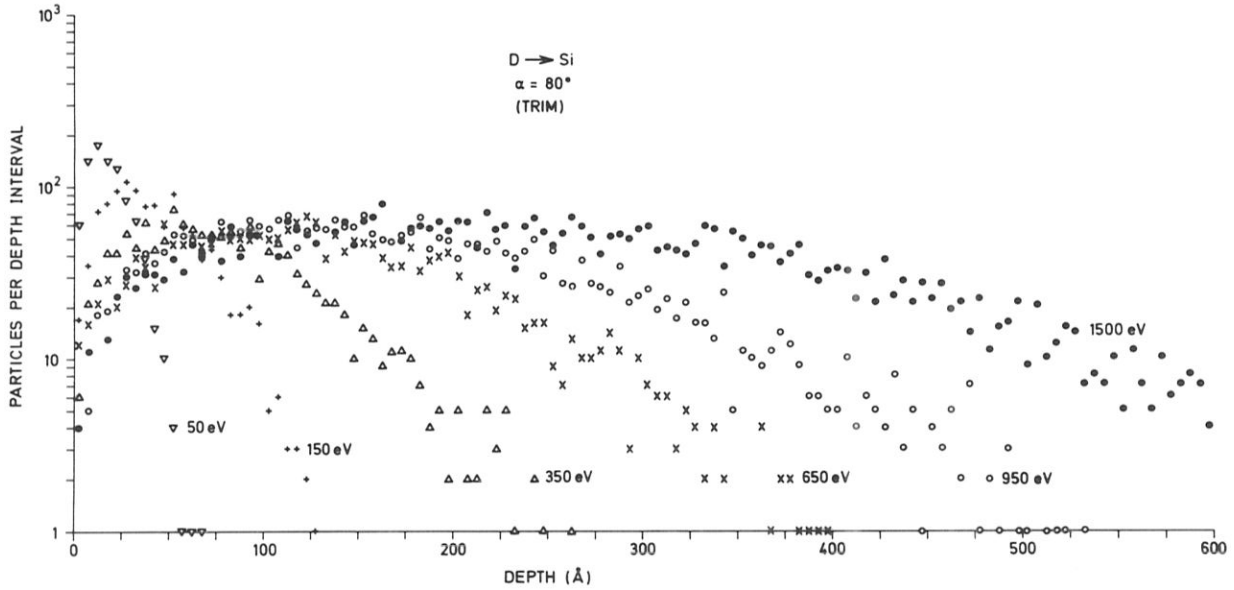

Fig.6: Depth distributions of implanted D in Si for 6 incident energies and an angle of incidence $\alpha = 80^{o}$ (in respect to the surface normal). The number of incident particles are 20 000 for one incident energy, the depth interval is 5 Å. 1.7 x Oen-Robinson inelastic energy loss was assumed.

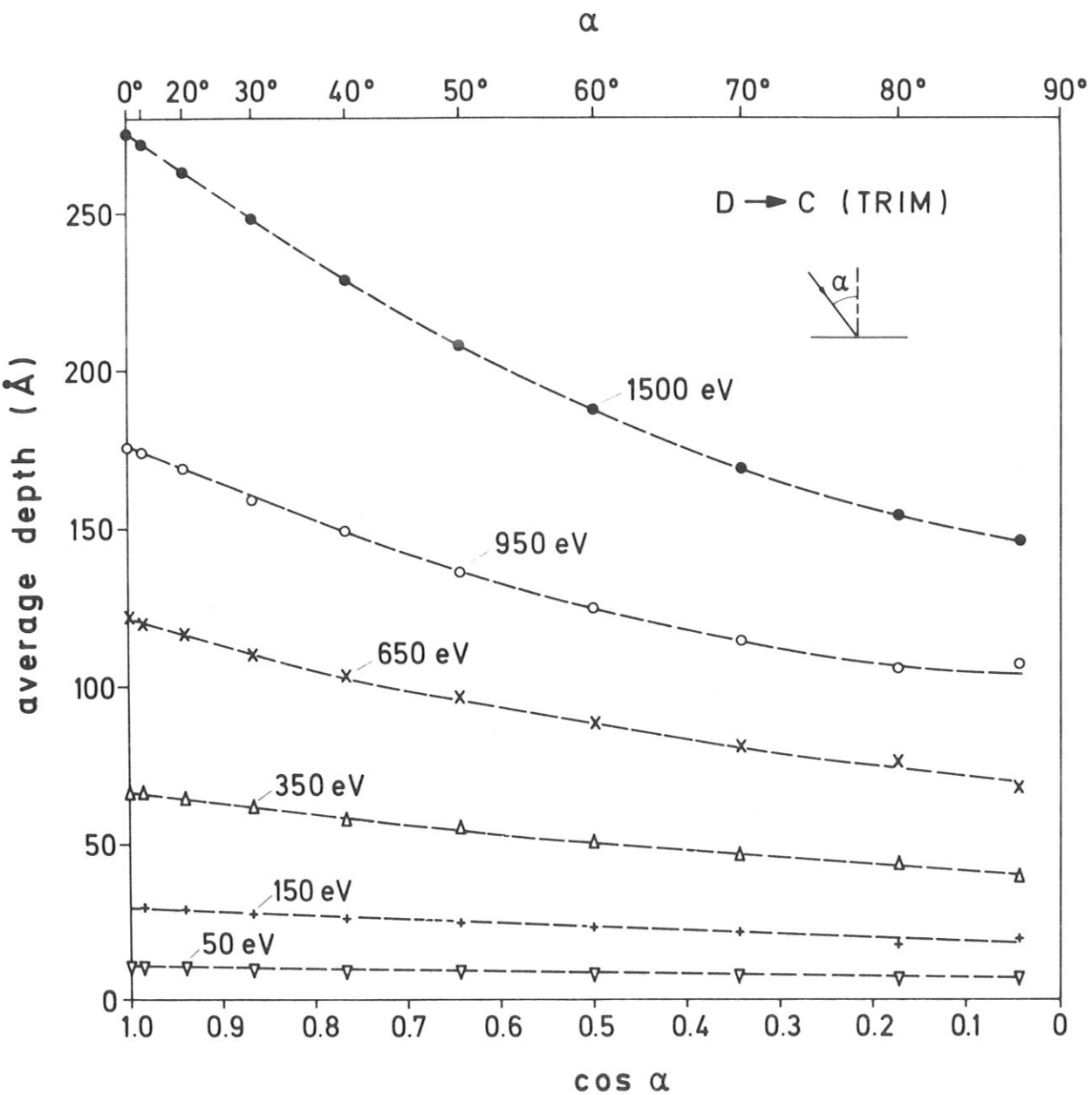

Fig.7: Dependence of the average depth (mean projected range) versus cosα for D onto C for 6 incident energies. Lindhard inelastic energy loss was assumed. Lines are drawn to guide the eye.

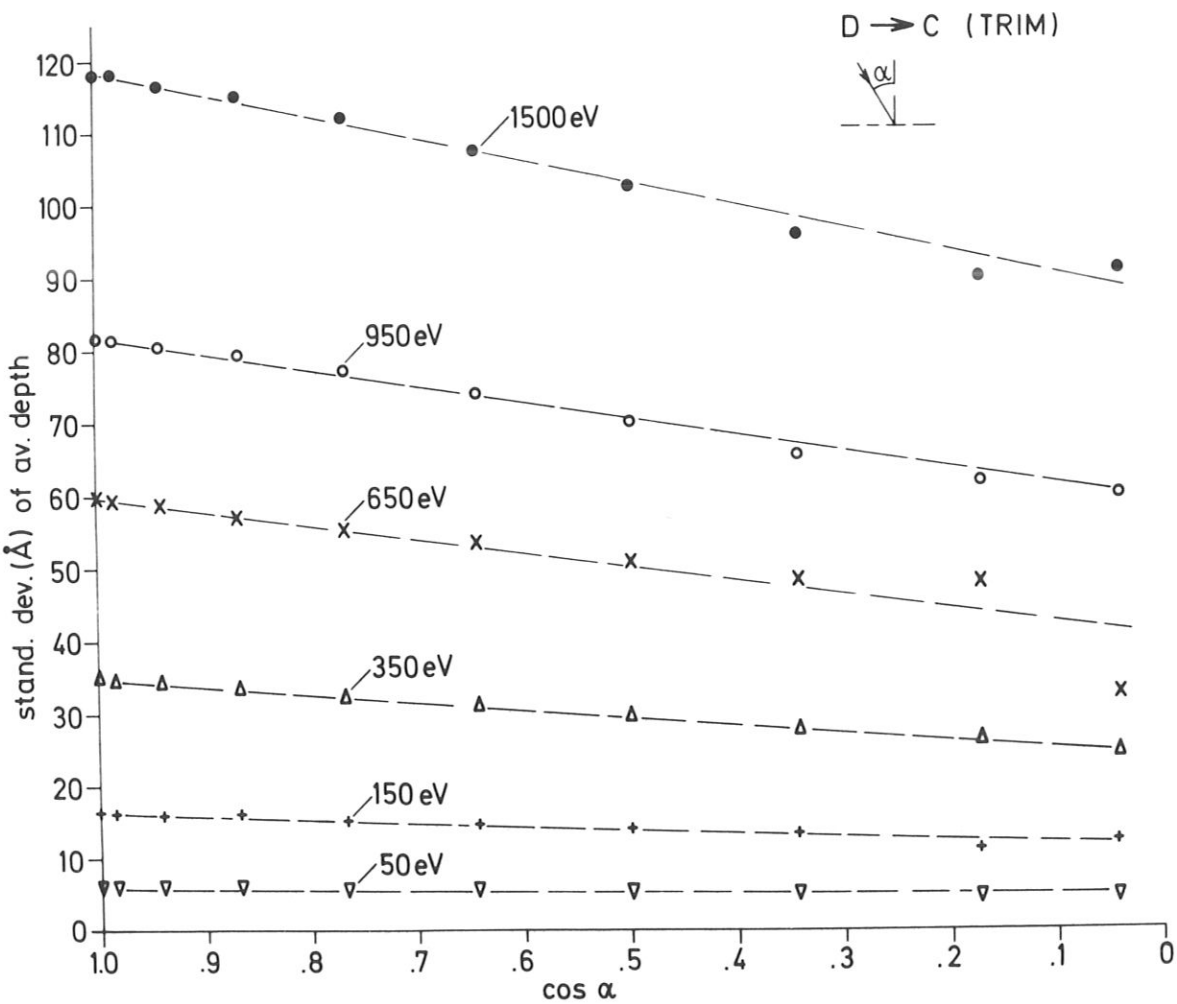

Fig.8: Dependence of the standard deviation of the average depth versus cosα for D onto C for 6 incident energies. Lindhard inelastic energy loss was assumed. Lines are drawn to guide the eye.

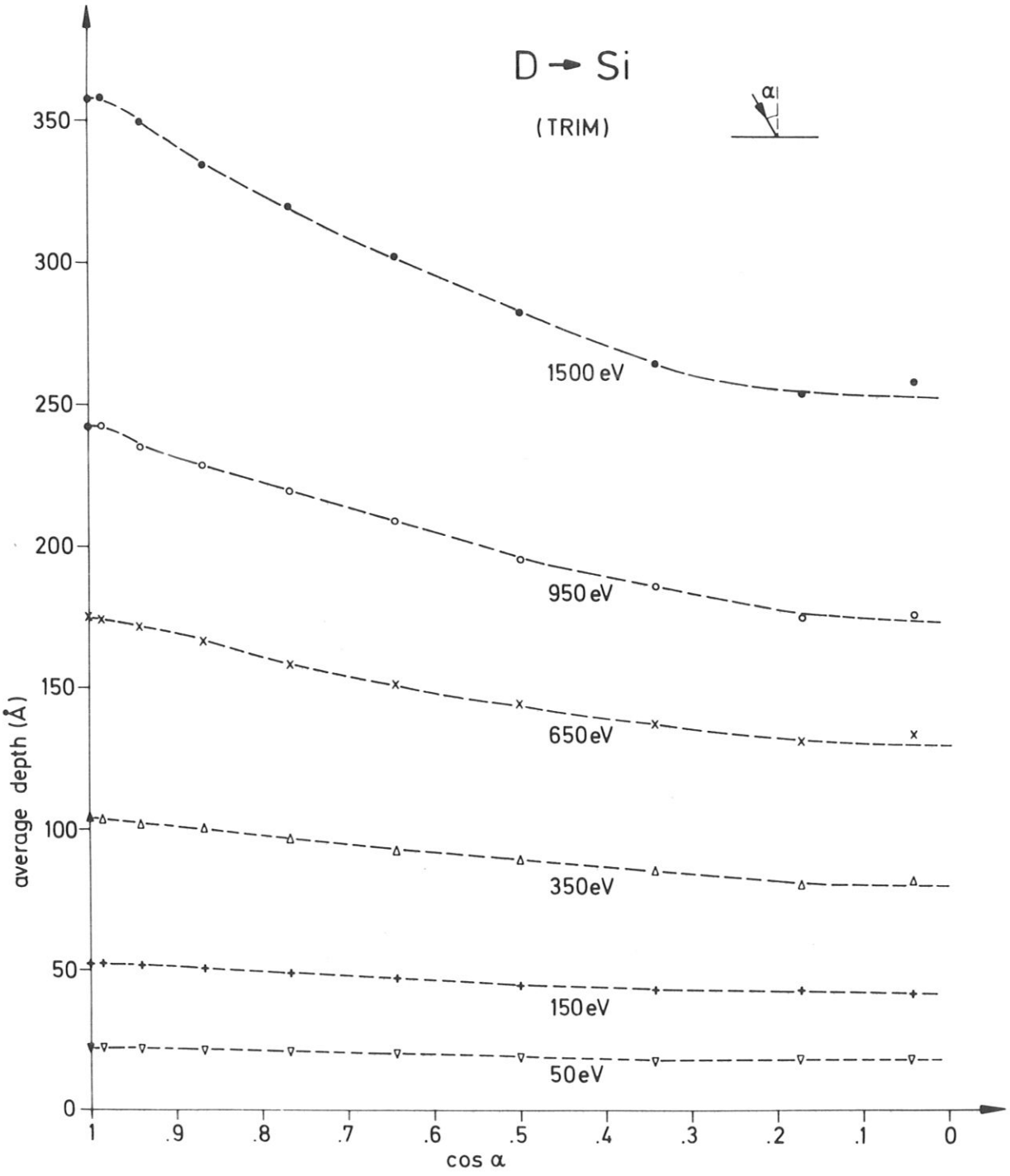

Fig.9: Dependence of the average depth (mean projected range) versus cosα for D onto Si for 6 incident energies. 1.7 x Oen-Robinson inelastic energy loss was assumed. Lines are drawn to guide the eye.

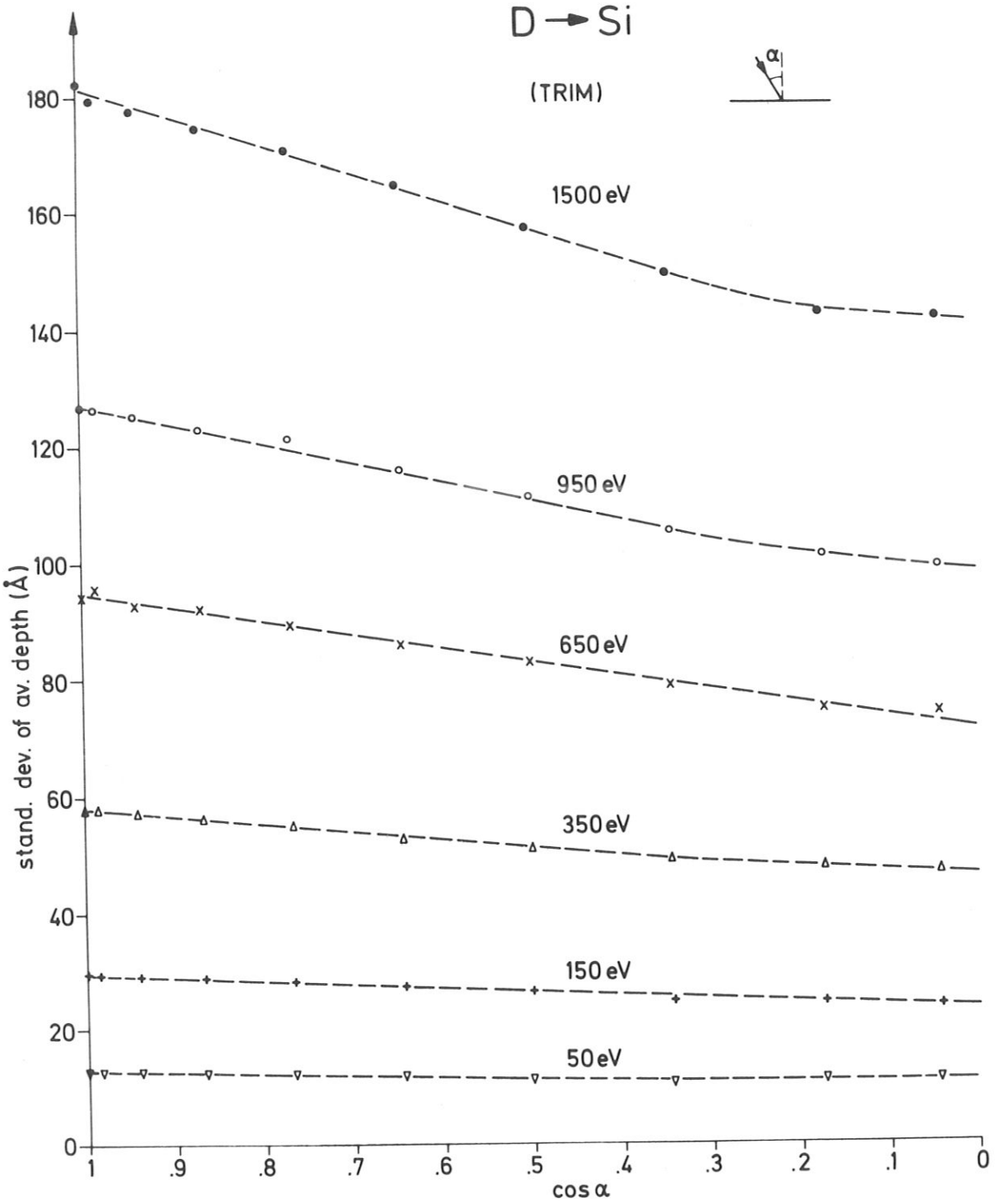

Fig.10: Dependence of the standard deviation of the average depth versus cosα for D onto Si for 6 incident energies. 1.7 x Oen-Robinson inelastic energy loss was assumed. Lines are drawn to guide the eye.

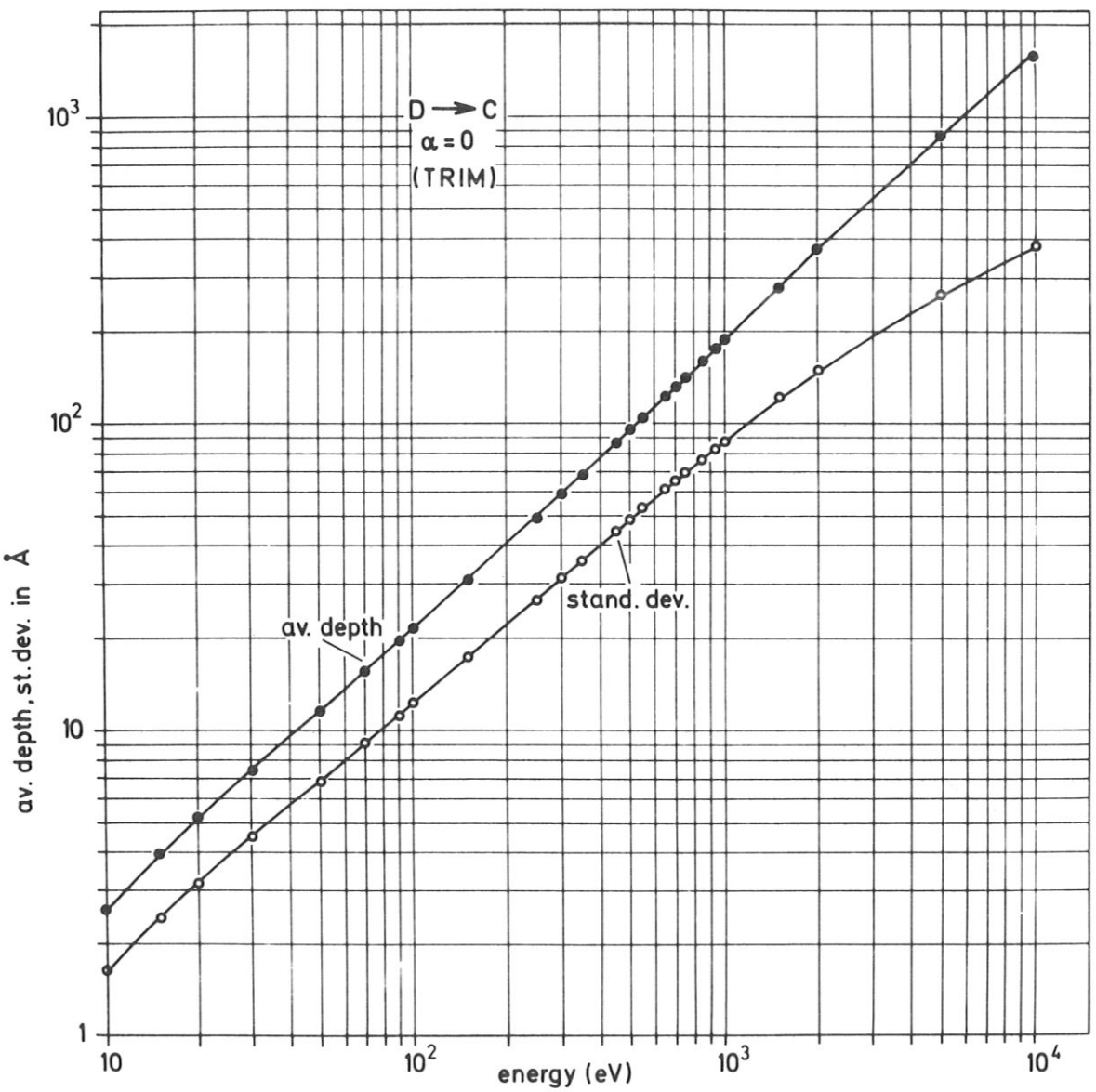

Fig.11: Average depth (mean projected range) and standard deviation of the average depth versus the incident energy of D onto C for normal incidence. Lindhard inelastic energy loss was assumed.

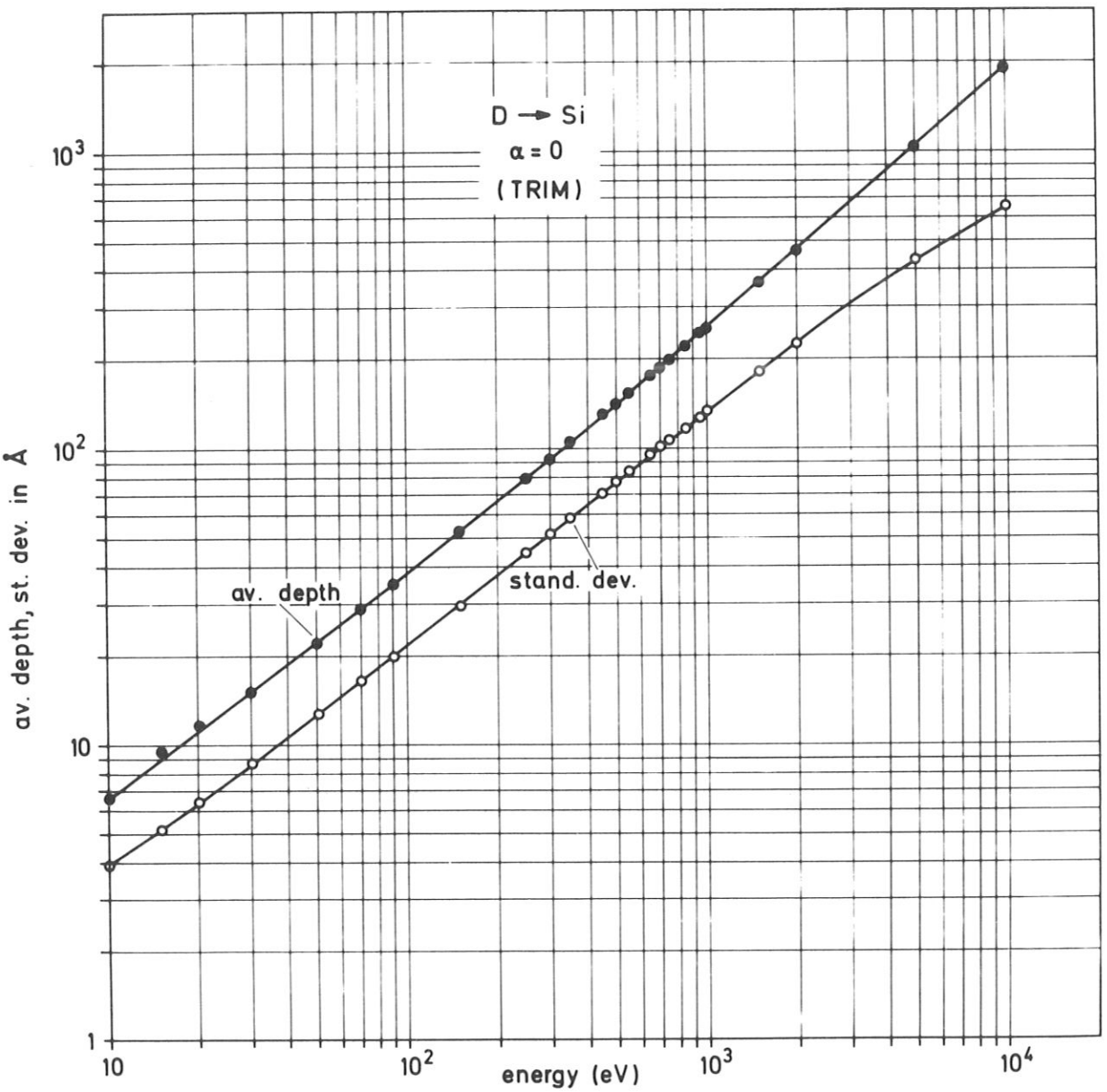

Fig.12: Average depth (mean projected range) and standard deviation of the average depth versus the incident energy of D into Si for normal incidence. 1.7 x Oen-Robinson inelastic energy loss was assumed.

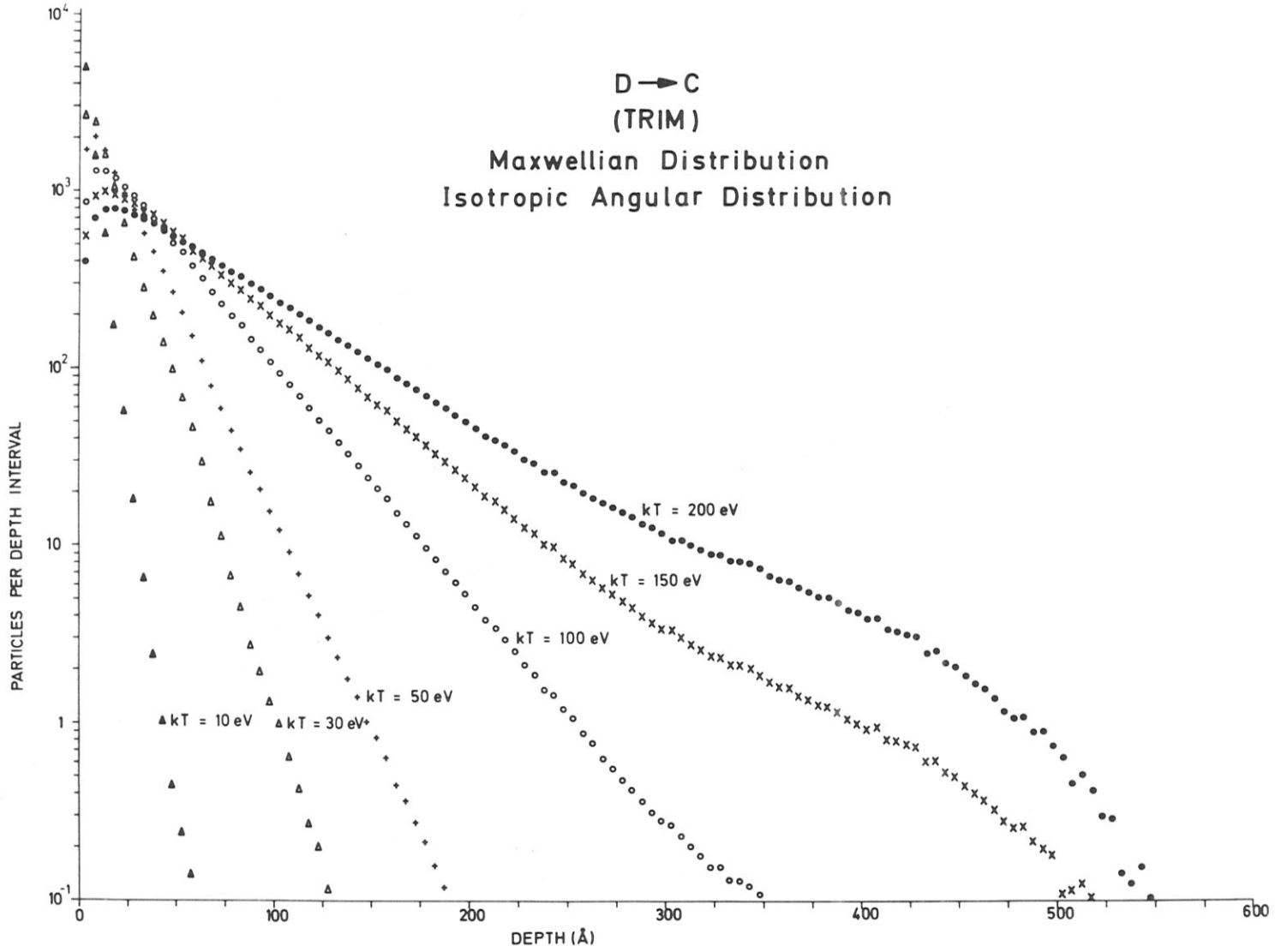

Fig.13: Trapped deuterium particles in a 5 Å depth interval in C for 6 plasma temperatures. 3 x 10^6 incident particles, Lindhard inelastic energy loss, Maxwellian energy distribution and isotropic angular distribution of the incident particles.

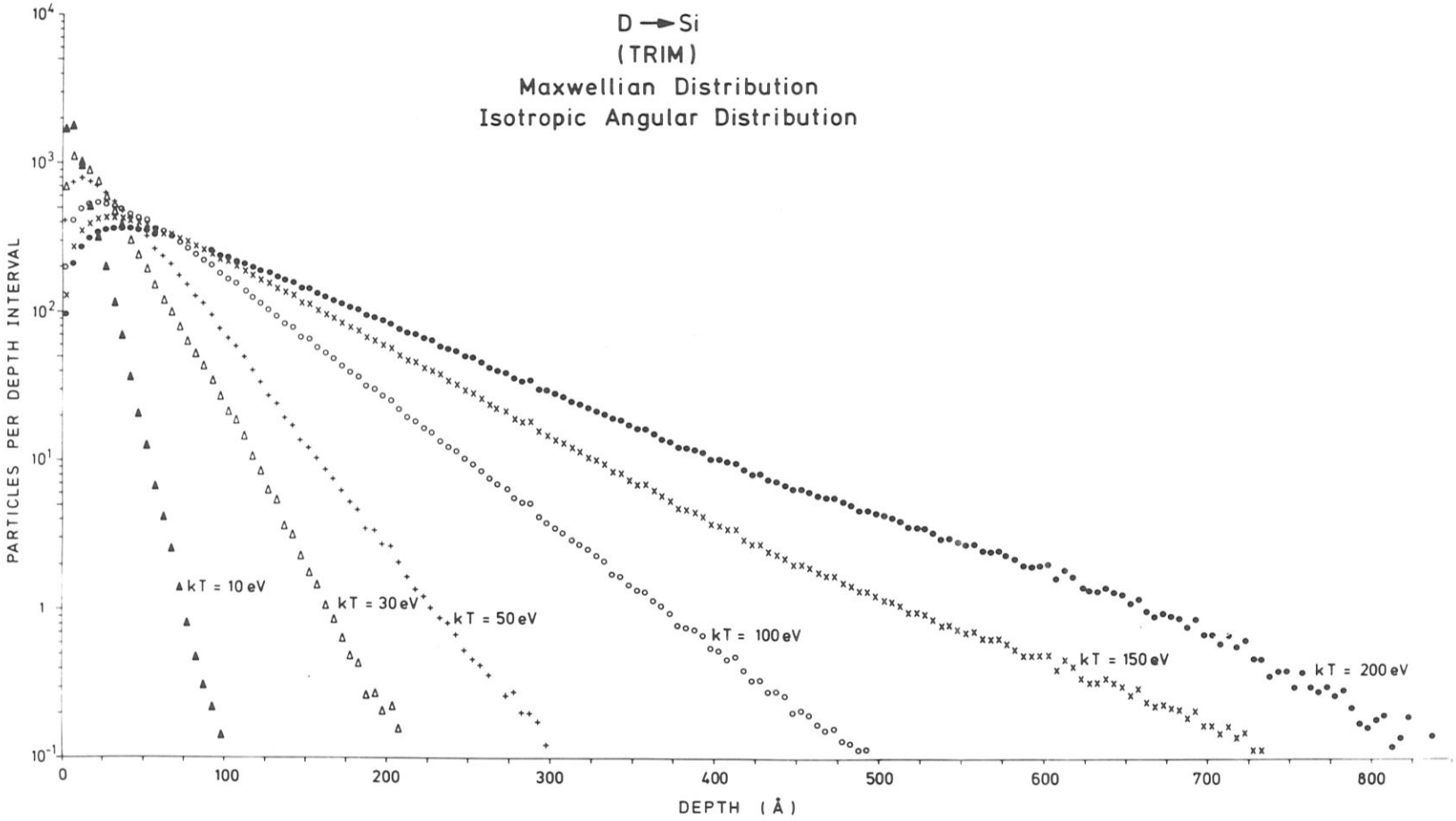

Fig.14: Trapped deuterium particles in a 5 Å depth interval in Si for 6 plasma temperatures. 3 x 10^6 incident particles. 1.7 x Oen-Robinson inelastic energy loss, Maxwellian energy distribution and isotropic angular distribution of the incident particles.

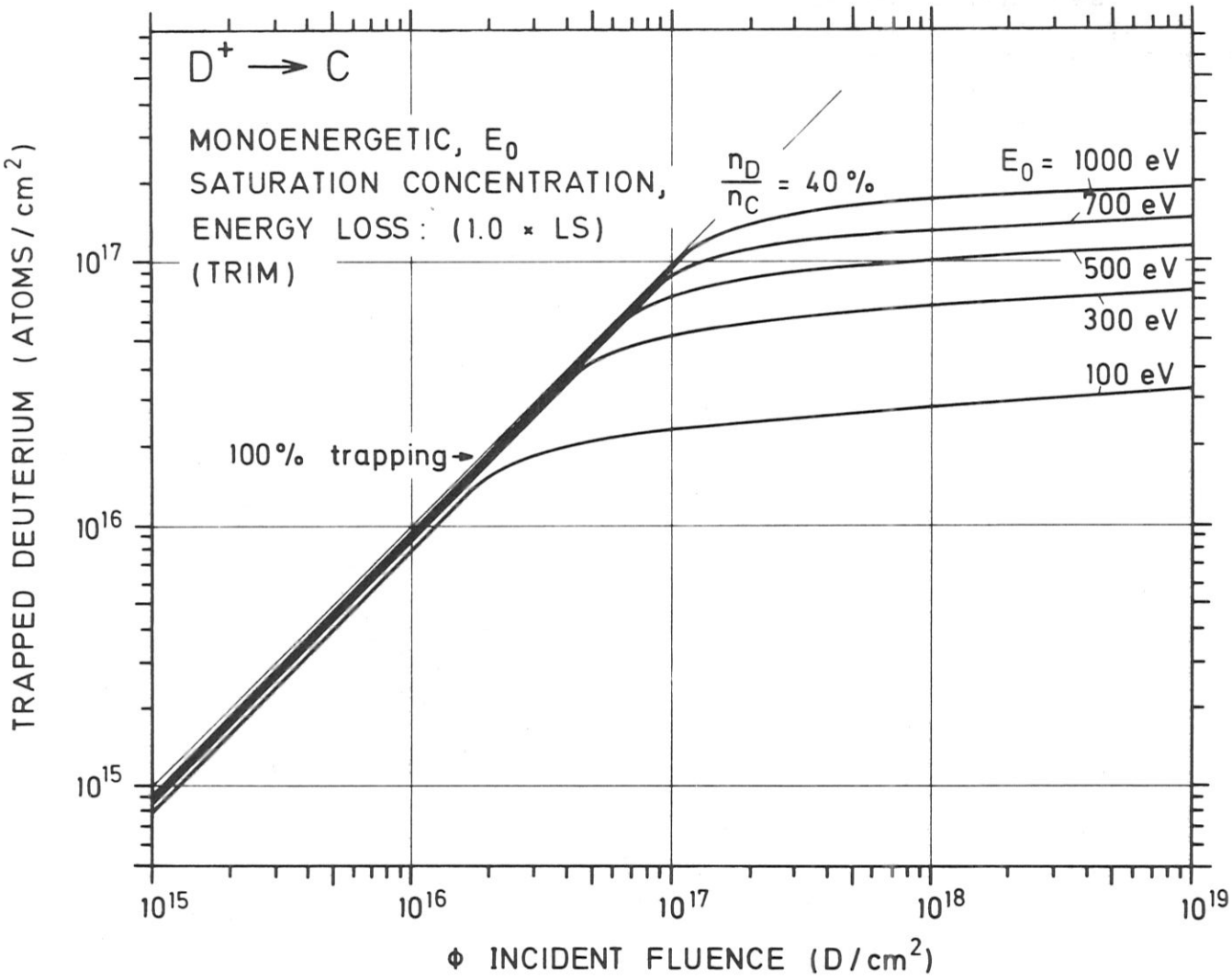

Fig.15: Trapped deuterium versus the incident fluence for D into C. Trapping curves are shown for 5 incident energies, normal incidence and a 40 % saturation concentration of D in C. 20 000 incident particles, Lindhard inelastic energy loss.

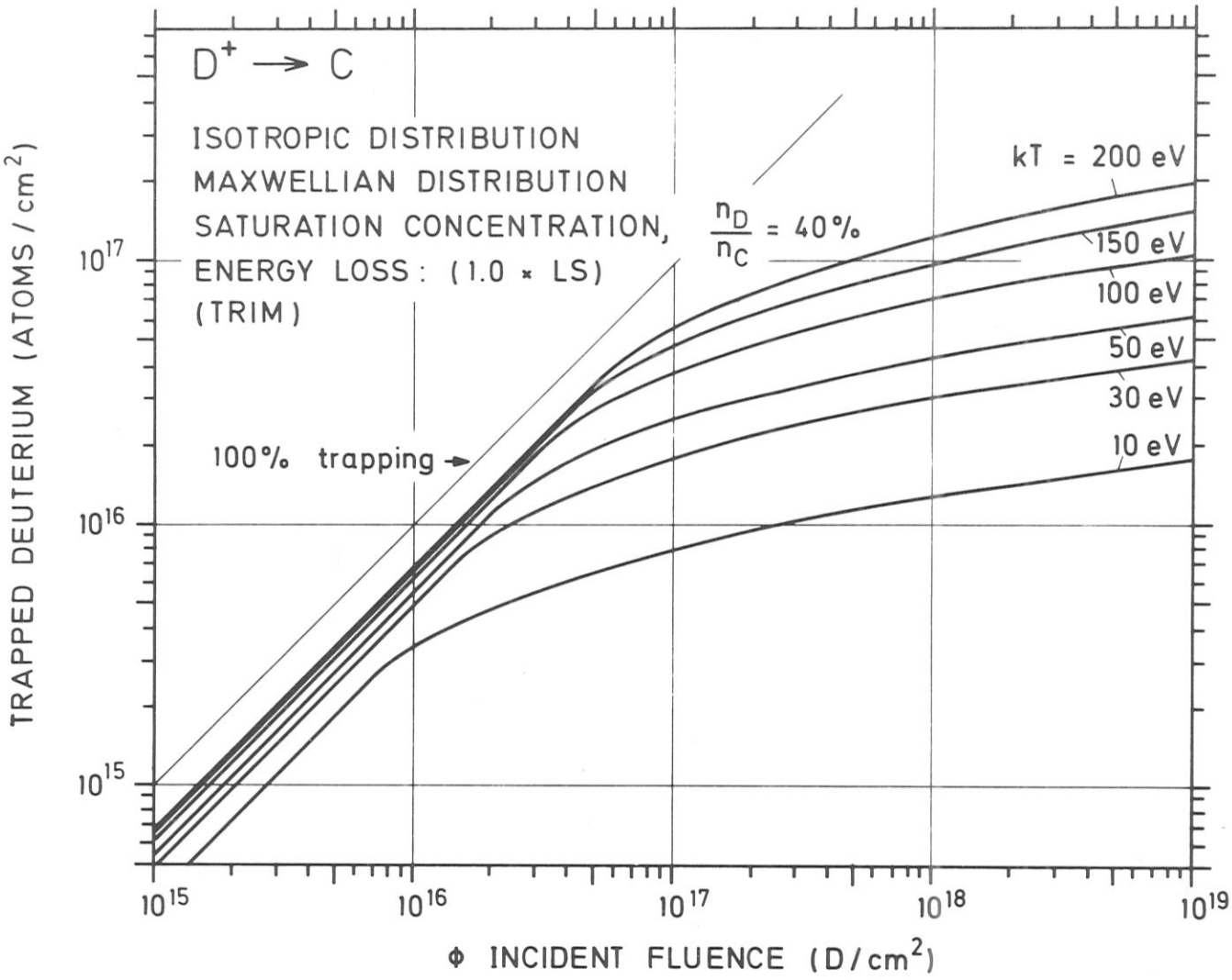

Fig.16: Trapped deuterium versus the incident fluence for D into C. Trapping curves are shown for 6 plasma temperatures, for a Maxwellian energy distribution and an isotropic angular distribution of the incident particles and for a saturation concentration of 40 % of D in C. 3×10^6 incident particles, Lindhard inelastic energy loss.

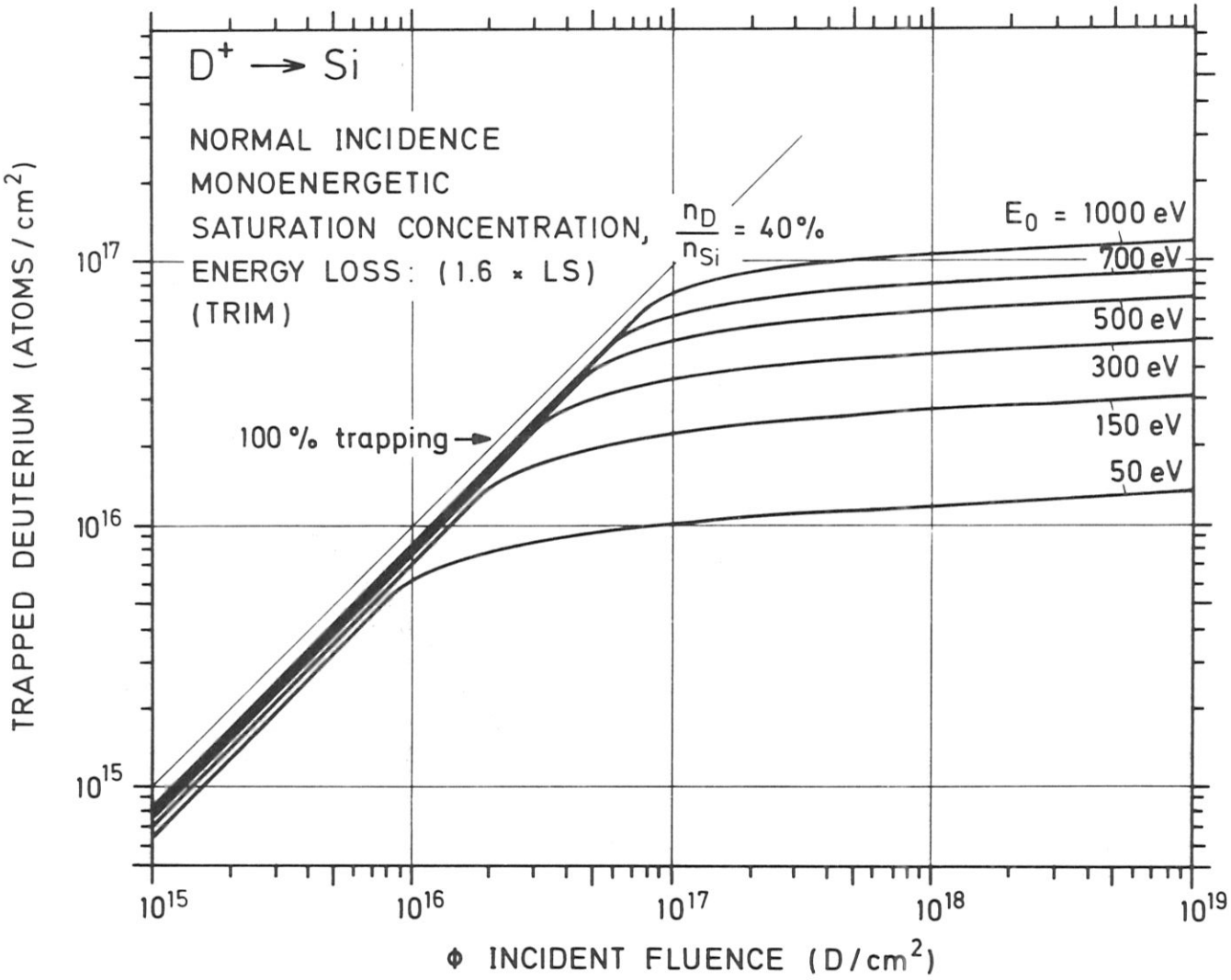

Fig.17: Trapped deuterium versus the incident fluence for D into Si. Trapping curves are shown for 6 incident energies, normal incidence and a 40 % saturation concentration of D in Si. 20 000 incident particles, 1.6 x Lindhard inelastic energy loss.

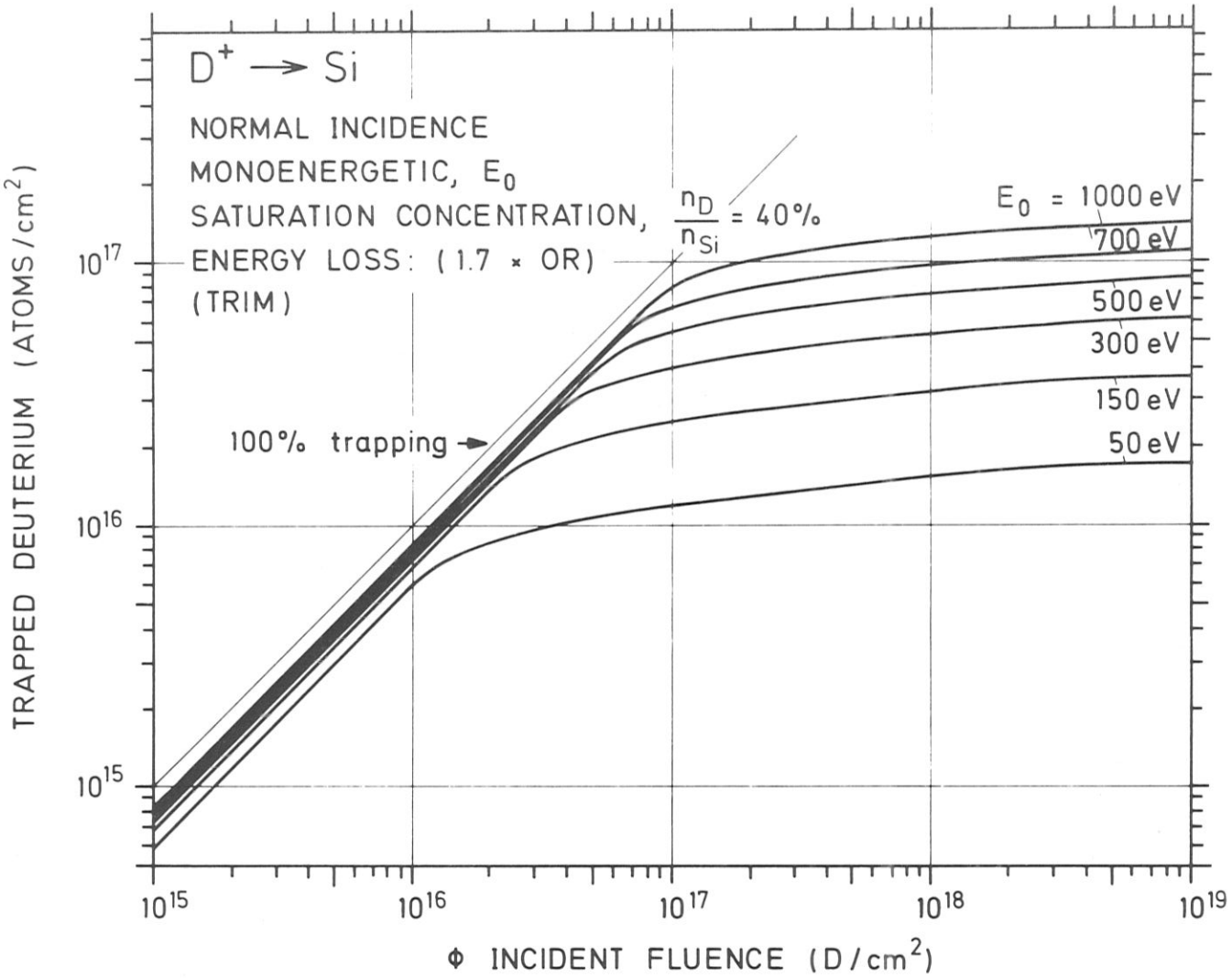

Fig.18: Trapped deuterium versus the incident fluence for D into Si. Trapping curves are shown for 6 incident energies, normal incidence and a 40 % saturation concentration of D in Si. 20 000 incident particles, 1.7 x Oen-Robinson inelastic energy loss.

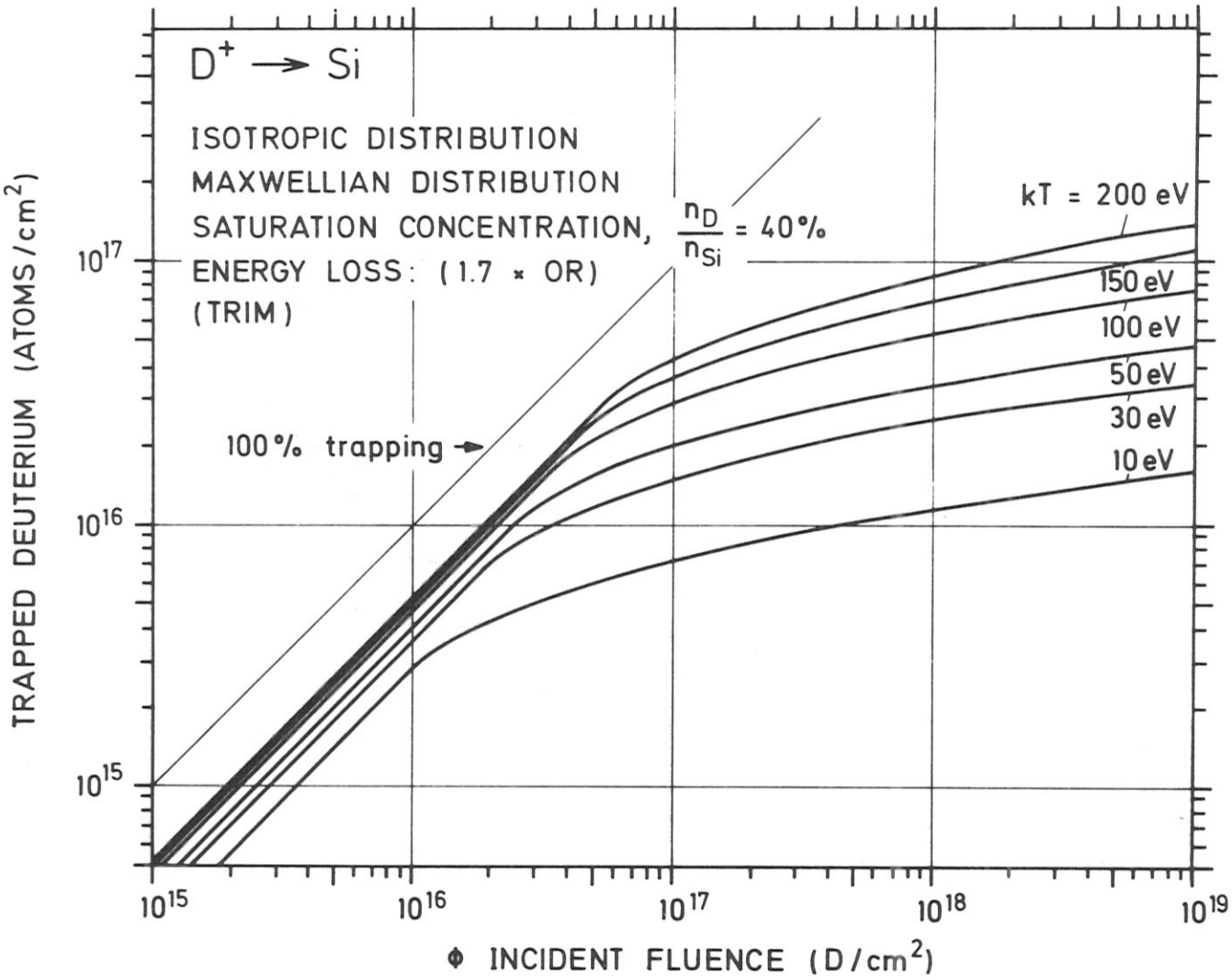

Fig.19: Trapped deuterium versus the incidence fluence for D into Si. Trapping curves are shown for 6 plasma temperatures, for a Maxwellian energy distribution and an isotropic angular distribution of the incident particles and for a 40 % saturation concentration of D in Si. 3 x 10^6 incident particles, 1.7 x Oen-Robinson inelastic energy loss.

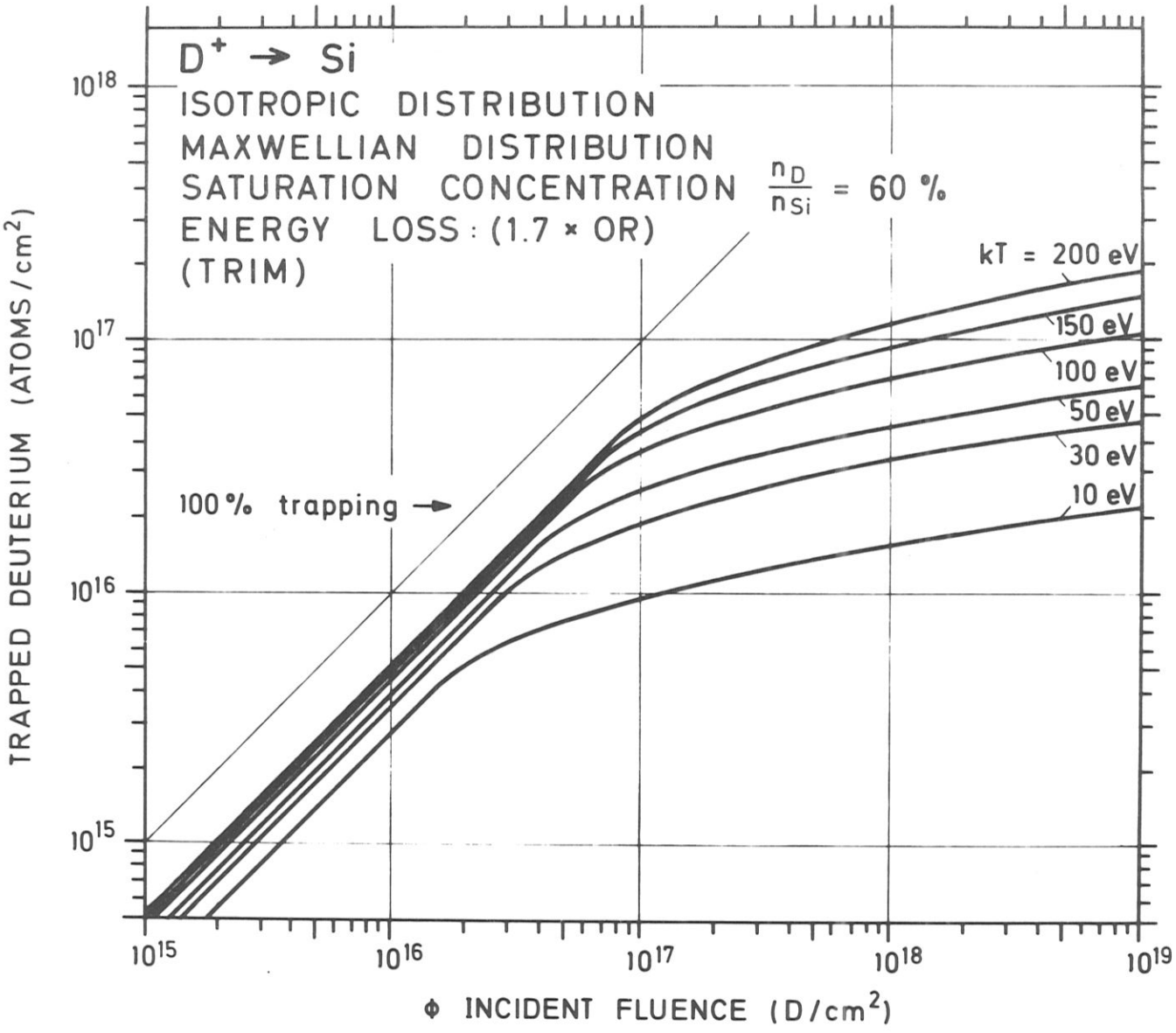

Fig.20: Trapped deuterium versus the incident fluence for D into Si. Trapping curves are shown for 6 plasma temperatures, for a Maxwellian energy distribution and an isotropic angular distribution of the incident particles and for a 60 % saturation concentration of D in Si. 3 x 10^6 incident particles, 1.7 x Oen-Robinson inelastic energy loss.

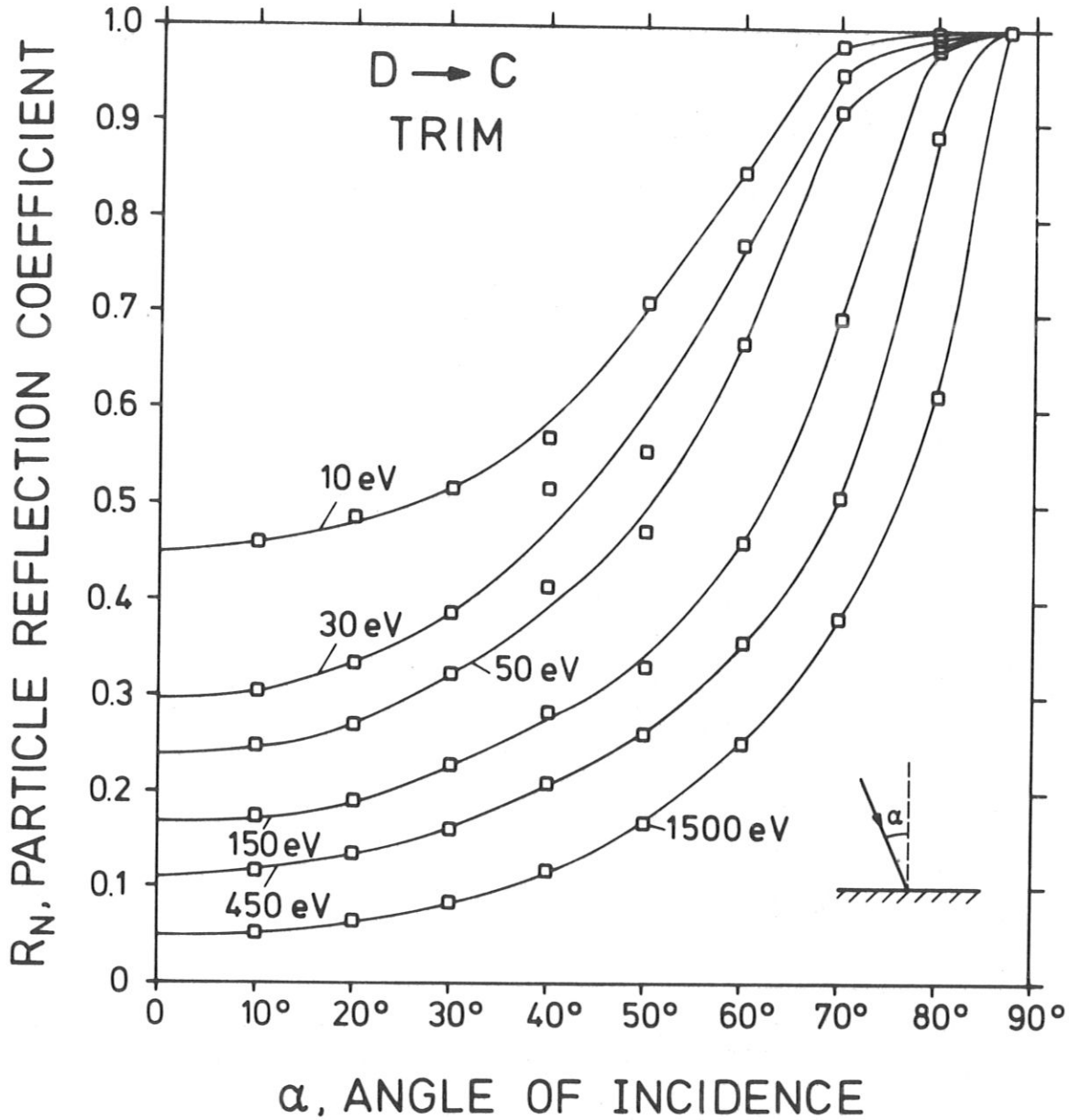

Fig.21: The particle reflection coefficient R_N versus the angle of incidence α for D onto C. 20 000 incident particles per incident energy and angle α, Lindhard inelastic energy loss.

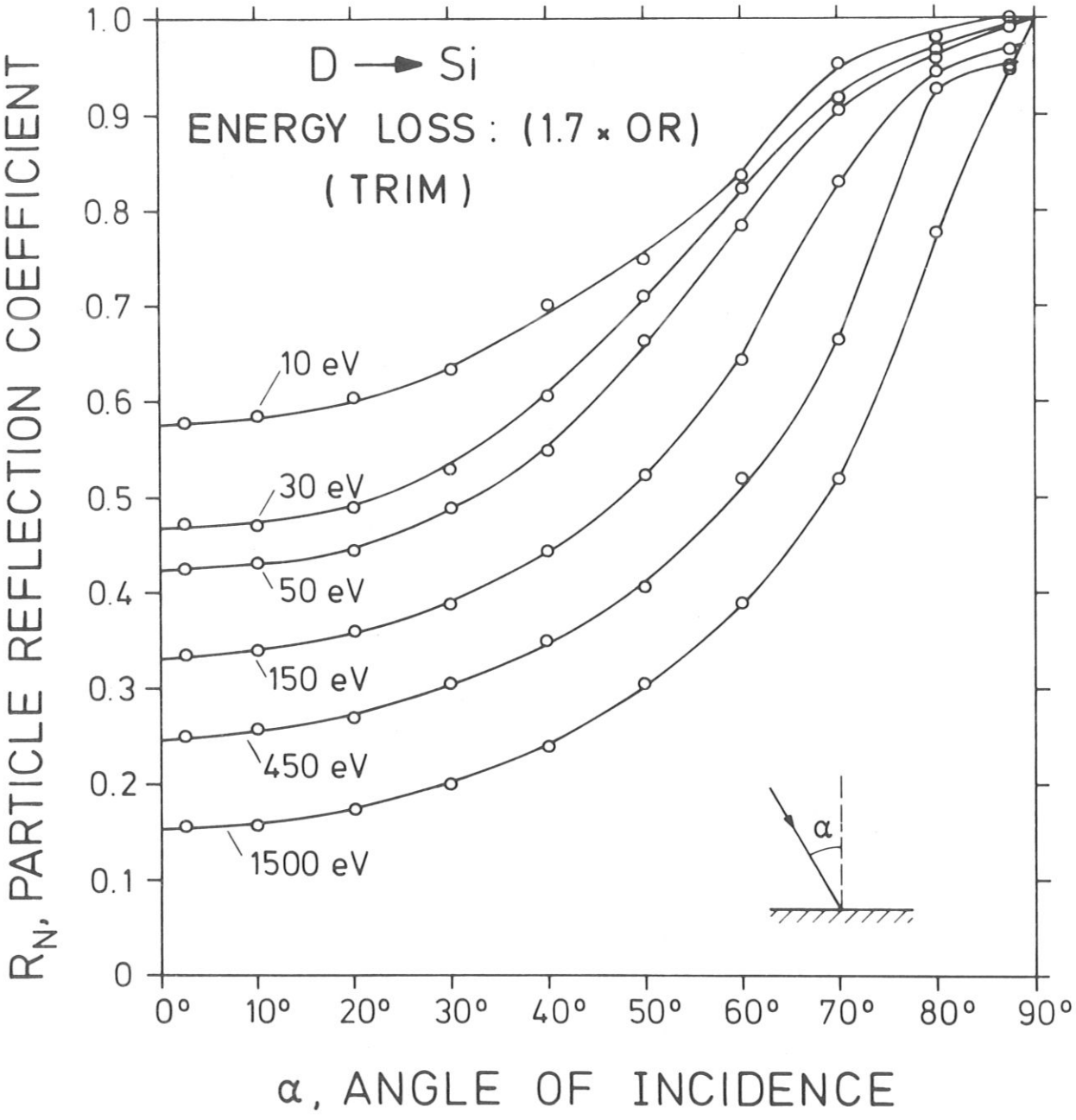

Fig.22: The particle reflection coefficient R_N versus the angle of incidence α for D onto Si. 20 000 incident particles per incident energy and angle α, 1.7 x Oen-Robinson inelastic energy loss.